Thermochimica Acta, 60 (1983) 265–275
Elsevier Scientific Publishing Company, Amsterdam – Printed in The Netherlands

HEAT CAPACITIES OF $NaNO_3$ AND KNO_3 FROM 350 TO 800 K

ROBERT W. CARLING

Sandia National Laboratories, Livermore, CA 94550 (U.S.A.)

(Received 28 May 1982)

ABSTRACT

The heat capacities of $NaNO_3$ and KNO_3 were determined from 350 to 800 K by differential scanning calorimetry. Solid–solid transitions and melting were observed at 550 and 583 K for $NaNO_3$ and 406 and 612 K for KNO_3, respectively. The entropies associated with the solid–solid transitions were measured to be (8.43 ± 0.25) J K^{-1} $mole^{-1}$ for $NaNO_3$ and (13.8 ± 0.4) J K^{-1} $mole^{-1}$ for KNO_3. At 298.15 K the values of C_p^0, S_T^0, $\{H^0(T) - H^0(0)\}/T$ and $-\{G^0(T) - H^0(0)\}/T$, respectively, are 91.94, 116.3, 57.73, and 58.55 J K^{-1} $mole^{-1}$ for $NaNO_3$ and 95.39, 133.0, 62.93, and 70.02 J K^{-1} $mole^{-1}$ for KNO_3. Values for S_T^0, $\{H^0(T) - H^0(0)\}/T$, and $-\{G^0(T) - H^0(0)\}/T$ were calculated and tabulated from 15 to 800 K for $NaNO_3$ and KNO_3.

INTRODUCTION

The use of molten nitrate salts as heat transfer fluids has engendered the need for reliable thermodynamic values to high temperature [1]. Previous heat capacity measurements [2–14] have been limited to slightly above the melting temperature. This work describes heat capacity results on $NaNO_3$ and KNO_3 from 350 to 800 K, substantially into the liquid regions of both salts. Heat capacity measurements determined in this study have been combined with low-temperature results reported by previous investigations to produce a complete set of thermodynamic functions from 15 to 800 K for both salts.

During the course of this investigation it was learned that the entropies associated with the solid–solid transitions in $NaNO_3$ and KNO_3 are uncertain. Although there have been numerous investigations on the thermodynamics of the fusion regions in $NaNO_3$ and KNO_3, very little has been done on the solid–solid transitions. Moreover, the results that are available do not agree. The uncertainties in the entropies of transition have led to several different interpretations of the mechanisms associated with the solid-state transitions. The results from this work were used to shed light on the nature of the transitions.

0040-6031/83/0000-0000/$03.00

EXPERIMENTAL

Heat capacity measurements were made with a Perkin-Elmer DSC-2 differential scanning calorimeter. All measurements were made with the samples sealed in gold or aluminum. Sapphire was used as the heat capacity reference material. Heat capacity measurements were made at a heating rate of 10° min^{-1} with range settings of 1.25–5.00 J min^{-1}. The $NaNO_3$ and KNO_3 were reagent grade material, recrystallized from water and dried at 425 K for at least 48 h in vacuum.

A Hewlett Packard 9825 desk-top calculator was used to control and operate the DSC. Measurements were typically taken over temperature ranges of 50–100°. Temperature ranges were overlapped and scanned several times resulting in heat capacities which are averages of several measurements (a minimum of three) at each temperature. Accuracies in the solid regions were estimated to be 2% by comparison with previous heat capacity results. The precisions in the liquid region are estimated to be 5%.

RESULTS AND DISCUSSION

The experimentally measured molar heat capacities for $NaNO_3$ and KNO_3 are given in Tables 1 and 2 and shown in Figs. 1 and 2. These results are in excellent agreement with previous measurements [4,5,7–13,15,16] up to the melting points. The agreement is much poorer in the liquid region and reasons for discrepancies will be discussed below.

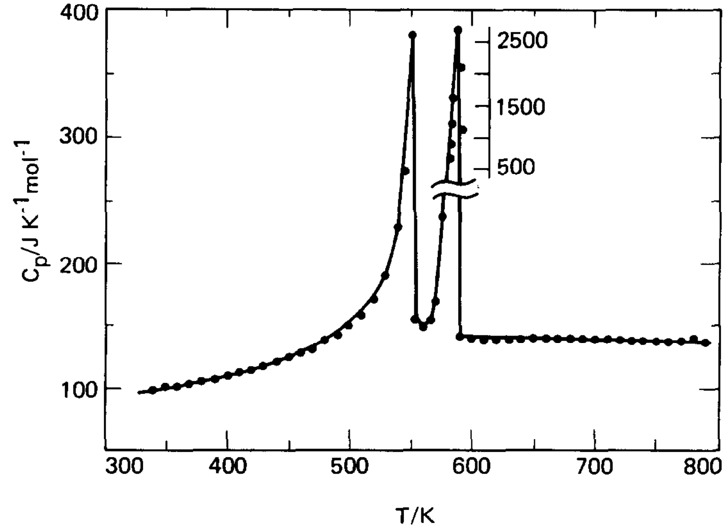

Fig. 1. Experimental heat capacity of $NaNO_3$.

TABLE 1

Heat capacities of $NaNO_3$

T (K)	C_p (J K^{-1} mole^{-1})	T (K)	C_p (J K^{-1} mole^{-1})	T (K)	C_p (J K^{-1} mole^{-1})
340	98.97	536	213.9	578	669.7
350	100.6	537	218.1	579	900.7
360	102.6	538	222.8	580	1231
370	105.0	539	227.8	581	1650
380	107.2	540	233.7	582	2195
390	109.4	541	239.2	583	2694
400	111.3	542	246.1	584	2624
410	114.0	543	254.3	585	2134
420	116.0	544	263.0	586	1137
430	118.5	545	273.8	587	178.1
440	121.8	546	286.0	588	144.0
450	125.1	547	302.7	589	142.2
460	128.2	548	324.8	590	139.0
470	132.7	549	359.3	600	140.2
480	138.0	550	380.7	610	139.9
490	142.9	551	193.3	620	140.5
500	150.1	552	165.8	630	139.5
510	158.7	553	159.1	640	140.4
520	173.3	554	156.0	650	141.0
521	175.0	559	151.3	660	142.9
522	176.8	564	152.9	670	142.8
523	178.7	565	154.0	680	140.9
524	180.7	566	155.9	690	141.0
525	182.6	567	158.4	700	140.7
526	185.0	568	161.2	710	140.4
527	187.1	569	164.9	720	138.8
528	189.4	570	169.4	730	138.9
529	191.9	571	175.7	740	139.0
530	194.4	572	184.0	750	134.4
531	196.8	573	195.6	760	133.1
532	200.4	574	212.2	770	133.9
533	203.3	575	238.1	780	137.1
534	206.6	576	305.1	790	143.4
535	210.3	577	479.9		

Thermodynamic functions were calculated for $NaNO_3$ and KNO_3 and the results are presented in Tables 3 and 4. Heat capacity values used to derive these functions were taken from three sources. Above 340 K, the heat capacity values determined experimentally in this study were used. Between 15 and 340 K, the results of Southard and Nelson [6] were used. Below 15 K, heat capacities were extrapolated using the Debye T^3 limiting law from which entropy and enthalpy increments were obtained. Within the transition

TABLE 2

Heat capacities of KNO_3

T (K)	C_p ($J K^{-1} mole^{-1}$)	T (K)	C_p ($J K^{-1} mole^{-1}$)	T (K)	C_p ($J K^{-1} mole^{-1}$)
330	96.01	420	123.7	611	2571
340	97.84	430	123.1	612	2923
350	99.04	440	123.6	613	2691
360	100.7	470	125.2	614	347.0
370	103.7	480	125.8	615	146.0
380	106.7	490	126.3	616	140.5
390	108.4	500	126.8	617	140.4
400	111.3	510	127.8	618	139.2
401	113.8	520	128.5	619	139.2
402	118.9	530	128.8	620	139.4
403	129.4	540	130.1	630	140.0
404	449.9	550	131.4	640	139.8
405	1544	560	132.9	650	140.3
406	2271	570	136.0	660	140.0
407	1263	580	139.1	670	139.1
408	183.3	590	139.4	680	137.6
409	130.4	600	140.1	690	136.8
410	127.0	601	141.0	700	136.5
411	125.9	602	141.2	710	135.7
412	125.6	603	141.2	720	135.7
413	124.9	604	141.6	730	135.3
414	125.1	605	141.9	740	136.4
415	124.8	606	145.3	750	136.2
416	124.6	607	151.4	760	135.8
417	124.6	608	171.2	770	134.5
418	124.5	609	618.6	780	132.2
419	124.2	610	1677	790	130.9

and melting regions, a different method of calculation was required because of the rapidly changing curvature. The heat capacities were fitted to polynomials in temperature by the method of least squares, and integrated to yield smoothed values of the thermodynamic functions at selected temperature intervals. The thermal functions in the vicinity of the transitions are based on numerical integration of heat-capacity points read from a plot of the transition and melting regions. The thermodynamic values are based on molar masses of 84.995 and 101.107 g $mole^{-1}$ for $NaNO_3$ and KNO_3, respectively.

The melting point and enthalpy of fusion were found to be 583 K and (15.1 ± 0.4) kJ $mole^{-1}$ for $NaNO_3$ and 612 K and (10.5 ± 0.3) kJ $mole^{-1}$ for KNO_3. These results are in excellent agreement with the recommended values given by Janz et al. [2].

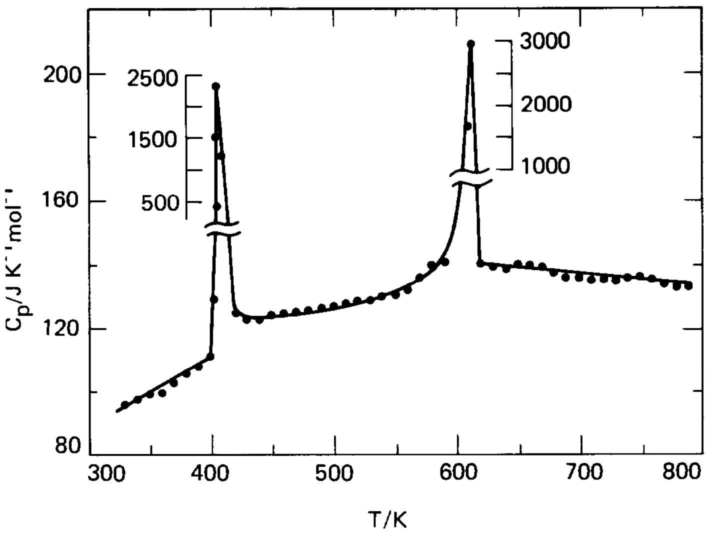

Fig. 2. Experimental heat capacity of KNO_3.

Liquid heat capacity

The heat capacities of liquid $NaNO_3$ and KNO_3 have previously been measured up to 675 K for both salts. This study extends the experimental data to 800 K. Experiments beyond this temperature were attempted but the results are not reported here because the decomposition pressure caused the sample pans to crack and salt to leak out.

Previous studies into the liquid region were either not very accurate or did not extend far enough into the liquid region to allow heat capacities to be determined with much confidence. Most previous work had assumed a constant heat capacity in the liquid, although some very recent work evinced a rapidly increasing heat capacity with values just past the melting points of 160–170 J K^{-1} $mole^{-1}$ for $NaNO_3$ and KNO_3 [13]. Unfortunately, few details are presented on the experimental technique so the reliability of the results cannot be assessed. Based on the measurements in this work and those of others a rapidly increasing heat capacity of such magnitude is unreasonable. As seen in Figs. 1 and 2 the heat capacity tends to decrease slightly as temperature increases in contrast to the constant heat capacity assumed by others. However, it is acknowledged that the apparent decrease is probably within the level of uncertainty in the data. The precision in the liquid region increased from about 2% to 5% from the melting points to 800 K.

Solid–Solid transitions

Solid–solid transitions were observed in $NaNO_3$ and KNO_3 at 550 and 406 K, respectively. Temperatures, enthalpies, and entropies associated with

TABLE 3

Standard molar thermodynamic functions of $NaNO_3$

T (K)	C_p ($J\ K^{-1}\ mole^{-1}$)	$S^0(T)-S^0(0)$ ($J\ K^{-1}\ mole^{-1}$)	$\{H^0(T)-H^0(0)\}/T$ ($J\ K^{-1}\ mole^{-1}$)	$-\{G^0(T)-H^0(0)\}/T$ ($J\ K^{-1}\ mole^{-1}$)
15	1.482	(0.500)	(0.373)	(0.127)
20	3.546	1.189	0.891	0.298
25	6.363	2.271	1.693	0.578
30	9.680	3.718	2.742	0.958
35	13.26	5.477	3.987	1.490
40	16.94	7.488	5.376	2.112
45	20.63	9.697	6.867	2.830
50	24.30	12.06	8.427	3.634
100	51.80	38.62	24.20	14.43
150	65.77	62.41	35.84	26.57
200	76.21	82.83	44.69	38.14
250	84.55	100.8	51.85	48.91
298.15	91.94	116.3	57.73	58.55
300	92.23	116.8	57.94	58.91
350	100.7	131.7	63.42	68.26
400	111.3	145.8	68.72	77.07
450	125.6	159.7	74.21	85.48
500	150.1	174.0	80.34	93.66
550 [a]	380.7			
583 [b]	2694			
600	139.1	231.4	120.8	110.6
650	142.3	242.7	122.4	120.4
700	139.1	253.2	123.7	129.5
750	136.7	262.7	124.6	138.1
800	142.5	271.6	125.5	146.1

[a] Peak of transition.

[b] Peak of melting.

the transitions are summarized in Table 5. The lattice heat capacities in the transition regions were deduced from graphical extrapolations of effective θ_D (lattice). These values of θ_D (lattice) were converted to lattice heat-capacity values to evaluate the excess enthalpy and entropy. The total enthalpies and entropies of the transitions and meltings were obtained from the difference between the integrated experimental heat-capacity curve and the estimated lattice contribution.

$NaNO_3$

At room temperature, $NaNO_3$ has the rhombohedral calcite structure. On heating, $NaNO_3$ undergoes what is most commonly regarded as a λ-type

TABLE 4

Standard molar thermodynamic functions of KNO_3

T (K)	C_p J K^{-1} $mole^{-1}$)	$S^0(T)-S^0(0)$ (J K^{-1} $mole^{-1}$)	$\{H^0(T)-H^0(0)\}/T$ (J K^{-1} $mole^{-1}$)	$-\{G^0(T)-H^0(0)\}/T$ (J K^{-1} $mole^{-1}$)
15	2.670	(0.810)	(0.609)	(0.201)
20	4.918	1.834	1.360	0.474
25	8.807	3.328	2.441	0.886
30	13.50	5.341	3.887	1.454
35	18.46	7.794	5.614	2.180
40	23.35	10.58	7.528	3.053
45	28.03	13.60	9.548	4.056
50	32.45	16.79	11.62	5.168
75	49.53	33.57	21.74	11.83
100	60.34	49.45	30.18	19.27
150	71.85	76.34	42.36	33.99
200	79.94	98.17	50.74	47.38
250	87.77	116.8	57.35	59.43
298.15	95.39	133.0	62.93	70.02
300	95.55	133.5	63.13	70.41
350	98.76	148.4	67.94	80.52
400	111.3	162.4	72.56	89.89
406 [a]	2271			
450	124.3	189.6	89.59	99.97
500	126.7	202.8	93.18	109.6
550	131.7	215.0	96.42	118.6
600	140.1	226.9	99.75	127.2
612 [b]	2923			
650	139.1	255.1	118.8	136.3
700	137.3	265.3	120.2	145.1
750	135.1	274.7	121.2	153.5
800	130.1	283.3	122.0	161.3

[a] Peak of transition.

[b] Peak of melting.

gradual transition with a transition temperature of 550 K as determined in this research. However, it has been argued that it is not possible to decide whether the $NaNO_3$ transition is a sluggish first-order or a second-order transition [20]. Using high pressure differential thermal analysis measurements, Klement [21–23] was able to convincingly describe the transition of $NaNO_3$ as a λ type. The work reported here further substantiates the transition of $NaNO_3$ as a second-order, λ-type transition. For λ transitions the variation of entropy with temperature, at constant pressure, should reach a point of inflection at the transition temperature [24,25]. Figure 3 shows this

TABLE 5

Thermodynamic properties of transitions in $NaNO_3$ and KNO_3

Compound	T_t (K)	ΔH_t (kJ mole^{-1})	ΔS_t (J K^{-1} mole^{-1})	Ref.
$NaNO_3$	550	4.42±0.13	8.43±0.25	This work
	549	3.95	5.27	7
	549.2	0.73±0.63	1.3 ±1.3	15
	549	4.3		17
	550	1.3		18
KNO_3	406	5.64±0.17	13.8 ±0.4	This work
	402	5.42		8
	401	5.10±0.02		11
	403	5.02		17
	400.6	4.98		19

to be the case and thus verifies the transition in $NaNO_3$ to be a λ-type, second-order transition.

Much debate in the literature has centered on the nature of the transition in $NaNO_3$. The transition was originally considered to have corresponded to the onset of free rotation of the nitrate ion [26,27]. However, since the entropy gain at the transition is small and the vibration–libration spectra do not show much change, it has been concluded that there is not free rotation of the NO_3^- ions in the high temperature phase [24]. If the NO_3^- ion does not rotate freely in the high temperature solid phase it must assume different orientations to account for the transition. X-Ray diffraction results suggest that because of the symmetry of the attractive field produced by the sodium ions the nitrate groups must occupy special positions in the unit cell. These special positions lead to a distribution of NO_3^- ions in calcite- and aragonite-like environments in the crystal structure of the high-temperature phase. Based on this interpretation Stromme [28] calculated a configurational entropy assuming the NO_3^- ions in the disordered phase are statistically distributed between the calcite- (45%) and aragonite-type (55%) structures. This model leads to a calculated entropy of transition of (7.95 ± 0.63) J K^{-1} mole^{-1}. The entropy of transition determined in this work is (8.43 ± 0.25) J K^{-1} mole^{-1}, in reasonable agreement with the theoretical value, and supports Stromme's model. By integrating C_p/T vs. T Stromme arrived at entropies of transition of 9.6, 7.1, and 9.6 J K^{-1} mole^{-1} from the heat capacity results of Sokolov and Shmidt [10], Mustajoki [7], and Reinsborough and Wetmore [4], respectively. These results give an average value of 8.8 J K^{-1} mole^{-1} agreeing reasonably well with the calculated value. Mustajoki [7], however, determined an entropy of transition of 5.27 J K^{-1}

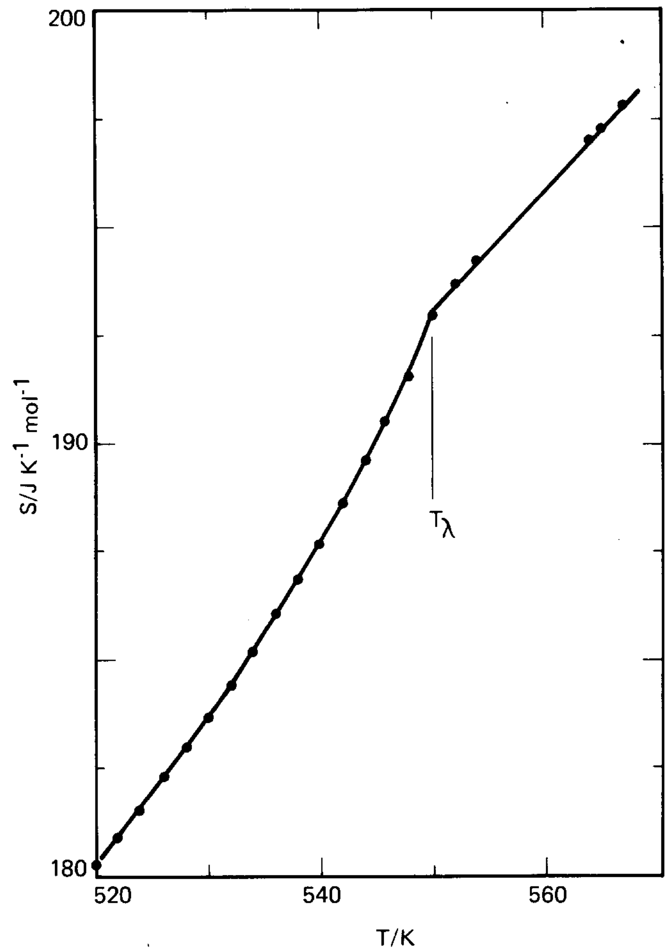

Fig. 3. Variation of entropy with temperature at λ-point in $NaNO_3$.

mole^{-1} (cf. Table 3). The reason for the discrepancy between Mustajoki's value and that calculated by Stromme using Mustajoki's data is unknown.

KNO_3

The solid–solid transition in KNO_3 involves a discontinuous change from one crystal structure (orthorhombic, phase II) to another (rhombohedral, phase I) at 406 K. In contrast to the behavior observed for $NaNO_3$, this transition is first order. Despite the different crystal structures Stromme [29] made an analysis on KNO_3 similar to that on $NaNO_3$ and calculated a configurational entropy change of (8.54 ± 0.54) J K^{-1} mole^{-1}. The result from this study (13.8 ± 0.4 J K^{-1} mole^{-1}) as well as values calculated from previous studies (13.5 ± 0.4 and 12.4 ± 0.1 J K^{-1} mole^{-1}) [8,19] do not agree with Stromme's value. This difference is ascribed to factors such as changes in vibrational state in the isothermal transition [29] in contrast to the gradual transition in $NaNO_3$.

Possible mechanisms for the movement of the nitrate ion at the transition and details are described by Newns and Slavely [27]. Briefly, the first mechanism describes phase I as having two possible off-center positions of the nitrate ion in the rhombohedral cell combining with each of two minima lying each side of a position where the oxygen atoms are in the same plane as one set of cations. This interpretation results in a phase I configurational entropy of $R \ln 4$ (11.5 J K^{-1} $mole^{-1}$). The other mechanism describes the nitrate ion as occupying six positions in phase I. This would result in a configurational entropy of $R \ln 6$ (14.9 J K^{-1} $mole^{-1}$) [30]. The transition entropy measured here, i.e. (13.8 ± 0.4) J K^{-1} $mole^{-1}$, is reasonably close to $R \ln 6$ and lends credence to the above interpretation on the nature of the transition.

ACKNOWLEDGEMENT

This work was supported by the U.S. Department of Energy, DOE, under Contract DE-AC04-76DP00789.

REFERENCES

1 K.W. Battleson, Solar Power Tower Design Guide, Solar Thermal Central Receiver Power Systems. A Source of Electricity and/or Process Heat, Sandia National Laboratories, SAND 81-8005, April 1981.

2 G.J. Janz, C.B. Allen, N.P. Bansal, R.M. Murphy and R.P.T. Tompkins, Physical Properties Data Compilations Relevant to Energy Storage. II. Molten Salts: Data on Single and Multi-Component Salt Systems, NSRDS–NBS 61, April 1979.

3 T.B. Douglas, Trans. ASME, 79 (1957) 23.

4 V.C. Reinsborough and F.E.W. Wetmore, Aust. J. Chem., 20 (1967) 1.

5 H.M. Goodwin and H.T. Kalmus, Phys. Rev., 28 (1909) 1.

6 J.C. Southard and R.A. Nelson, J. Am. Chem. Soc., 55 (1933) 4865.

7 A. Mustajoki, Ann. Acad. Sci. Fenn., Ser. A6, (5) (1957).

8 A. Mustajoki, Ann. Acad. Sci. Fenn., Ser. A6, (99) (1962).

9 V.A. Sokolov, V.A. Palkin and N.E. Shmidt, Izv. Sekt. Fiz. Khim. Anal., Inst. Obsch. Neorg. Khim., Akad. Nauk SSSR, 25 (1954) 134.

10 V.A. Sokolov and N.E. Shmidt, Izv. Sekt. Fiz. Khim. Anal., Inst. Obsch. Neorg. Khim., Akad. Nauk SSSR, 26 (1955) 123.

11 V.A. Sokolov and N.E. Shmidt, Izv. Sekt. Fiz. Khim. Anal., Inst. Obsch. Neorg. Khim., Akad. Nauk SSSR, 27 (1956) 217.

12 P. Nguyen-Duy and E.A. Dancy, Thermochim. Acta, 39 (1980) 95.

13 T. Asahina, M. Kosaka and H. Taoda, Nagoya Kogyo Gijutsu Shikensho Hokoku, 29 (1980) 25.

14 G.J. Janz, Molten Salts Handbook, Academic Press, New York, 1967, p. 200.

15 G.J. Janz, F.J. Kelly and J.L. Perano, J. Chem. Eng. Data, 9 (1964) 133.

16 K.K. Kelley, Contributions to the Data on Theoretical Metallurgy XIII, Bulletin 584, Bureau of Mines, 1960.
17 C.N.R. Rao, B. Prakash and M. Naturajan, Crystal Structure Transformations in Inorganic Nitrites, Nitrates, and Carbonates, NSRDS–NBS 53, May 1975.
18 E.A. Dancy and P. Nguyen-Duy, Thermochim. Acta, 31 (1979) 395.
19 A. Arell, Ann. Acad. Sci. Fenn., Ser. A6, (101) (1962).
20 E. Rapoport, J. Phys. Chem. Solids, 27 (1966) 1349.
21 W. Klement, Jr., J. Phys. Chem., 72 (1968) 1294.
22 W. Klement, Jr., J. Phys. Chem., 74 (1970) 2751.
23 W. Klement, Jr., J. Phys. Chem., 74 (1970) 2753.
24 C.N.R. Rao and K.J. Rao, Phase Transitions in Solids, McGraw-Hill, New York, 1978, p. 128.
25 A.B. Pippard, Elements of Classical Thermodynamics, Cambridge University Press, 1966, pp. 140–144.
26 F.C. Kracek, E. Posnjak and S.B. Hendricks, J. Am. Chem. Soc., 53 (1931) 3339.
27 D.M. Newns and L.A.K. Stavely, Chem. Rev., 66 (1966) 267.
28 K.O. Stromme, Acta Chem. Scand., 23 (1969) 1616.
29 K.O. Stromme, Acta Chem. Scand., 23 (1969) 1625.
30 E.F. Westrum, Jr., Pure Appl. Chem., 8 (1964) 187.